



Stress concentration at cruciform welded joints under axial and bending loading modes

Krzysztof L. Molski¹ · Piotr Tarasiuk¹ · Grzegorz Glinka²

Received: 5 November 2018 / Accepted: 15 July 2020 / Published online: 12 August 2020
© The Author(s) 2020

Abstract

The paper is concerned with the problem of stress concentration in cruciform fillet welded joints subjected to axial and bending load. Extended numerical analyses were carried out with the help of the finite element method. It made it possible to estimate stress concentration factors K_t for a variety of geometrical parameters defining the geometry of cruciform welded joints. It has been found that approximate K_t formulas, available in the literature, have two disadvantages, i.e. an unknown accuracy and small range of application with respect to geometrical parameters defining the weld shape. For these reasons, more general and accurate new formulas for stress concentration factors K_t have been derived. Even though the present approach is applicable to all types of welded joints, the analysis presented below has been conducted for a cruciform joint with the weld flank angle of $\theta = 45^\circ$. Final solutions have been given in the form of polynomial expressions, and they can be easily used in computer-aided design procedures.

Keywords Cruciform welded joints · Stress concentration factor · Weld geometry · Finite element method · Axial and bending load · Fillets

List of symbols

a	Weld throat thickness	2α	Total angle of the sharp corner
K_t	Theoretical elastic stress concentration factor	δ_x	Accuracy of the approximate K_t value
K_{tb}	Pure bending stress concentration factor	θ	Weld flank angle
K_{ta}	Pure axial stress concentration factor	κ	Correction function for the relative attachment thickness T/a
h	Attachment weld leg length	κ_b	Correction function for the relative attachment thickness T/a for pure bending load
h_p	Main plate leg length	κ_t	Correction function for the relative attachment thickness T/a for pure axial load
$n=\lambda-1$	Stress field exponent for a sharp corner	λ	Eigenvalue of the characteristic equation
N	Number of loading cycles	ρ	Weld toe radius
S	Cyclic stress	σ_b	Nominal bending stress
t	Thickness of the main plate	σ_t	Nominal axial stress
T	Thickness of the attachment plate		
$X=\rho/(\rho+a)$	Normalised weld toe radius parameter		
$Y=a/(a+t)$	Normalised weld thickness parameter		

Recommended for publication by Commission XV - Design, Analysis, and Fabrication of Welded Structures

✉ Piotr Tarasiuk
p.tarasiuk@pb.edu.pl

¹ Faculty of Mechanical Engineering, Bialystok University of Technology, Bialystok, Poland

² Mechanical and Mechatronics Engineering, University of Waterloo, Waterloo N0B 2H0, Canada

1 Introduction

The linear elastic stress concentration factor K_t is one of the most important parameters used in predicting fatigue life of structural components with various types of stress raisers like holes, notches, grooves, and stiffeners. A variety of K_t solutions and approximated formulas can be found in the literature (e.g. [1–7]). Welded joints are often used in engineering practice, but apart from their economic advantages, the

technological process involved possesses several additional problems which have to be considered in design procedures. The heat-affected zone, residual stresses, microstructural changes of the material and geometry of the weld-producing local non-uniform stress distribution are of great importance while predicting the fatigue strength and durability of such joints. The damage process usually initiates at the weld toe [8, 9], especially in the case of cruciform joints without the lack of penetration [10] or when the fillet weld size is sufficiently large [11]. Therefore, this region is of special interest to designers. From the point of view of the joint quality, it is important to predict the maximum permissible stresses at critical locations of the joint as well as to verify design requirements by means of measurable geometry parameters. The general form of a cruciform welded joint and its basic geometrical dimensions are shown in Fig. 1.

It is generally accepted [12, 13] that the overall load applied to the main plate of thickness t may be regarded as the superposition of the axial and bending load. For this reason, the maximum stress, appearing at critical locations, shown in Fig. 1 as circles, depends on both the axial and bending load magnitude, and it is described by two stress concentration factors K_{tt} and K_{tb} , respectively. These factors are usually defined as the ratio of the maximum peak stress to the nominal stress, often called the remote stress [14, 15] or as the average stress in the notch root cross section. Sometimes, the hot spot stress [12] is also used to define the stress concentration factor as well. Despite the fact that maximum stresses due to tension and bending are not located at the same point on the small curvilinear surface of the weld toe, they are close enough to consider the peak stress as being the sum of those two independent contributions. Since the stress concentration phenomenon depends on several geometrical parameters of the joint, the determination of the stress concentration factor K_t is a troublesome and time-consuming process. For practical engineering applications, various approximate formulas of K_t are used.

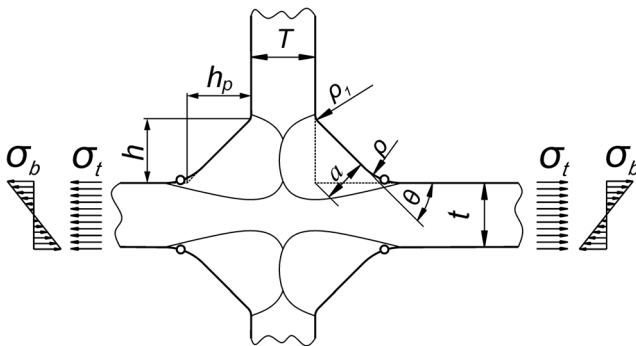


Fig. 1 Cruciform welded joint and its basic geometrical dimensions

2 Available stress concentration factor formulas for cruciform joints

A variety of approximate K_t formulas for welded joints can be found in the literature [12, 14–16]. Examples of such formulas, presented by Ushirokawa and Nakayama (U&N) [14] and Tsuji [16] for a cruciform joint subjected to axial and bending load, are shown below, Eqs. (1)–(3):

- axial load

Ushirokawa and Nakayama [14]:

$$K_{tt} = 1 + 2.2 \left[\frac{h/\rho}{2.8(W/t)-2} \right]^{0.65} \left\{ \frac{1 - \exp[-0.9\theta\sqrt{W/2h}]}{1 - \exp[-0.9(\pi/2)\sqrt{W/2h}]} \right\} \quad (1)$$

Tsuji [16]:

$$K_{tt} = 1 + \left[1.348 + 0.397 \ln \left(\frac{T + 2h_p}{t} \right) \right] \left[\frac{h/\rho}{2.8(W/t)-2} \right]^{0.467} \left\{ \frac{1 - \exp[-0.9\theta\sqrt{W/2h}]}{1 - \exp[-0.9(\pi/2)\sqrt{W/2h}]} \right\} \quad (2)$$

- bending load

Ushirokawa and Nakayama [14]:

$$K_{tb} = 1 + \sqrt{\tanh \left(\frac{2T}{t + 2h} + \frac{2\rho}{t} \right)} \left\{ \tanh \left[\frac{(2h/t)^{1/4}}{1 - \rho/t} \right] \right\} \left\{ \frac{0.13 + 0.65(1 - \rho/t)^4}{(\rho/t)^{1/3}} \right\} \left\{ \frac{1 - \exp[-0.9\theta\sqrt{W/2h}]}{1 - \exp[-0.9(\pi/2)\sqrt{W/2h}]} \right\} \quad (3)$$

where $W = (t + 4h) + 0.3(T + 2h_p)$ and θ is in radians.

All parameters appearing in formulas (1)–(3) are defined in Fig. 1.

Taking into account the typical shape and slope of the well-known fatigue S – N curve [17, 18], it is clear that the predicted fatigue life of a welded joint depends strongly on the accuracy of estimated K_t factors. Despite the fact that several authors were concerned mostly with

fatigue crack propagation life of such joints [11, 19, 20], the stress concentration factor K_t is also useful for estimating stress distributions in critical cross sections needed for fracture mechanics-based analyses [9, 13]. For this reason, extended numerical *FEM*-based analyses have been carried out to verify the range of validity and accuracy of available approximate K_t formulas (1)–(3) and to develop extended K_t formulas for a wider range of geometrical parameters.

3 Analysis of stress concentration factors by using the finite element method

3.1 General assumptions

The shapes and basic geometrical parameters of the full penetration cruciform welded joint are depicted in Fig. 1.

The following assumptions have been made:

1. Joint material is linear elastic, isotropic and homogeneous.
2. Small deformations occur due to external loading—tensile and bending.
3. Joint material is free from residual stresses, structural irregularities and imperfections including lack of penetration defects.
4. Weld faces are plane, and contour of the weldment is smooth, with a transition radius $\rho > 0$.
5. Weld flank angle $\theta = 45^\circ$.
6. Both attached plates are of the same thickness T and are co-linear.
7. Four welds are symmetrical.
8. K_{tt} for tensile and K_{tb} for bending loads are defined as $\sigma_{1\max}/\sigma_t$ and $\sigma_{1\max}/\sigma_b$, respectively.

3.2 The numerical model and boundary conditions

Numerical models of a variety of cruciform joint geometries have been developed using the ANSYS *FEM* program. Due to the double symmetry of the joint under axial load and symmetric-anti-symmetric deformation under bending load, only one quarter of the total joint was modelled. The geometry of the joint and the boundary conditions are schematically shown in Fig. 2.

The weld throat thickness parameter a was introduced for convenience, and it represents, in this case (for $\theta = 45^\circ$), the weld throat thickness, as shown in Figs. 1 and 2. The attachment leg length h and the main plate leg length h_p , shown in Fig. 1 and appearing in Eqs. (1)–(3), are related to the weld throat thickness a in the form of Eq. (4).

$$a = h\cos(\theta) = h_p\sin(\theta). \quad (4)$$

Equation (4) makes it possible to reduce the number of independent variables used in the analysis. In the present case ($\theta = 45^\circ$), the following relations hold $a = 0.707 h = 0.707 h_p$. Besides that, two non-dimensional parameters X and Y have been introduced in the form of expressions (5) and (6).

$$X = \rho/(\rho + a) = \frac{\rho/a}{\rho/a + 1} \quad (5)$$

$$Y = a/(a + t) = \frac{a/t}{a/t + 1} \quad (6)$$

The introduction of parameters X and Y makes further analysis more convenient than when directly using parameters ρ/a and a/t . In this way, all possible values of parameters X and Y fall into the range of 0, 1. For each particular geometrical case analysed in plane stress, a very fine mesh composed of about 800,000 linear PLANE182 finite elements was used. PLANE182 finite element is defined by 4 nodes having 2 degrees of freedom at each node. The mesh density was increased in the weld toe region where the number of finite elements along the arc, described by the toe radius ρ , was about 15 to 60, depending on the radius magnitude. In all cases, the geometrical proportions were selected in a way to obtain an unperturbed nominal stress field in a cross section located sufficiently far from the weld zone. At the initial stage of building the *FEM* model, the finite element mesh density was successively increased to obtain a stable numerical solution with the maximum stress value staying constant. As a result of gathering a significant number of cases and corresponding numerical solutions, a special mesh-generating procedure was developed. Moreover, the size of the finite elements changed smoothly the further from the zone of maximum stress concentration. These assumptions made the finite element mesh very fine.

The weld toe radius, ρ_1 , along the attachment weld line was arbitrarily chosen as $0.1a$, and it had no influence on stress concentration factors K_{tt} and K_{tb} . Relative lengths of the main and attachment plate, as well as the type of load and “rolling support” displacement boundary conditions, are shown schematically in Fig. 2. The thickness of the attachment plate, denoted as T in the present analysis, was normalised with respect to the weld throat thickness parameter a and varied within the range of $1 \leq T/a \leq 4$. The non-dimensional parameters X and Y have fallen into the range of 0.01 to 0.57 each. Particular values of stress concentration factors K_{tt} and K_{tb} were obtained by dividing the maximum peak stress at the weld toe by the nominal remote stress.

Number of finite elements, nodes and the minimum size of the element depended on the proportions between geometrical parameters of the joint represented by X , Y and T/a . For example, the model shown in

Fig. 2 Geometry and boundary conditions of the cruciform joint subjected to **a** axial load and **b** bending load

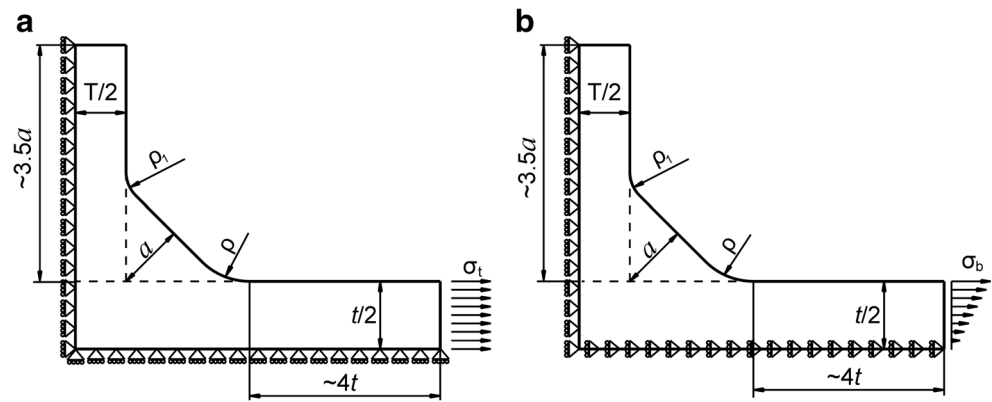


Fig. 3, where $X=0.2$, $Y=0.4$ and $T/t=1$, contained 872,642 elements and 875,096 nodes.

3.3 Accuracy of approximate K_t formulas

After performing the numerical calculations, approximate K_{tt} and K_{tb} values, given by formulas (1)–(3), were compared to those ones obtained with the help of the *FEM* method. Two examples of such comparisons obtained for the tensile and bending load are shown in Table 1 and Table 2, respectively. The accuracy δ_x is defined as the difference (%) between approximate K_t formulas (Eqs. (1)–(3)) and those obtained from the present *FEM* analysis and relative to the *FEM* data.

From the set of results presented in Table 1 and Table 2, one may conclude that the accuracy of stress concentration factors K_{tt} and K_{tb} obtained from approximate formulas (2) and (3) varies within the range of +12.3 to –22% and would give rather poor predictions of fatigue life. It appears that the approximate formulas have two important disadvantages: undetermined accuracy and narrow range of application with respect to geometrical parameters defining the weld geometry. For this reason, it seems necessary to elaborate on a slightly updated approach to the problem of stress concentration factors K_{tt} and K_{tb} in cruciform welded joints.

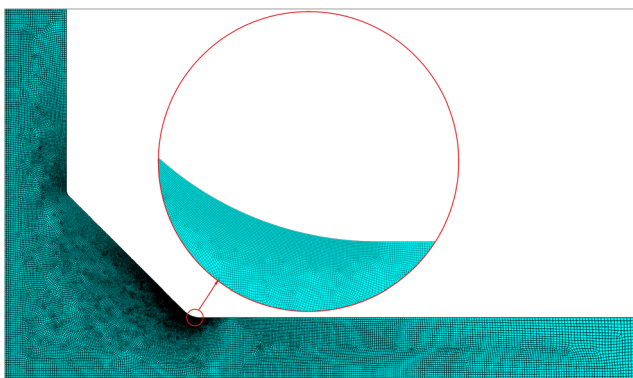


Fig. 3 Example of a finite element mesh for $X=0.2$, $Y=0.4$ and $T/t=1.0$

4 The weld toe radius and the plate thickness effects

It is important, while analysing the stress concentration phenomenon in welded joints with fillet welds, to know the effect of particular geometrical parameters on stress concentration factors K_{tt} and K_{tb} . Two typical situations appearing while designing welded structures are considered below. The first one is when only the weld toe radius ρ varies, and the second one is when only the main plate thickness t varies, while in both cases, all remaining parameters stay the same. It is worth noting that in both cases, the classical most important non-dimensional parameter ρ/t changes as well, and it tends to the limit zero when $\rho \rightarrow 0$ or $t \rightarrow \infty$. As a result, two different limit stress concentration factors occur for the value of $\rho/t \rightarrow 0$.

4.1 The weld toe radius effect

It is well-known that the weld toe radius ρ is the most important parameter influencing the stress concentration in a welded joint. Therefore, there are design requirements available preventing using notch tip radii smaller than the recommended limit.

Let us assume that the weld toe radius ρ varies, while all remaining geometrical parameters stay the same. The *FEM*-based stress concentration factors K_{tt} obtained in due course are shown in Fig. 4 in terms of the normalised parameter X . They were determined for several levels of parameter Y .

All curves (Fig. 4) are singular, which means that stress concentration factors increase rapidly when the weld toe root radius ρ approaches zero, while all other geometrical parameters of the joint do not vary. Such a behaviour needs special mathematical care when using approximate fitted expressions to capture variations of the stress concentration factor. In such cases, Eqs. (1) and (2) can be presented in the form of Eqs. (7) and

Table 1 Comparison of tensile stress concentration factors K_{tt} obtained with the *FEM* with those developed by Ushirokawa and Nakayama (U&N, Eq. (1)) and Tsuji (Eq. (2)), where $\theta = 45^\circ$, $h = h_p$, $t = T$, $h/t = 0.75$, $0.025 \leq \rho/t \leq 0.35$

	ρ/t	0.025	0.050	0.075	0.10	0.15	0.25	0.35
K_{tt}	<i>FEM</i>	3.768	3.013	2.649	2.420	2.137	1.838	1.673
	U&N	4.231	3.059	2.582	2.312	2.008	1.723	1.581
accuracy δ_x		+12.3%	+1.5%	-2.5%	-4.5%	-6.0%	-6.2%	-5.5%
K_{tt}	Tsuji	3.103	2.521	2.259	2.101	1.911	1.718	1.613
	accuracy δ_x		-17.6%	-16.3%	-14.7%	-13.2%	-10.6%	-6.5%

Table 2 Comparison of bending stress concentration factors K_{tb} obtained with the *FEM* with those developed by Ushirokawa and Nakayama (U&N Eq. (3)), where $\theta = 45^\circ$, $h = h_p$, $t = T$, $h/t = 0.75$, $0.025 \leq \rho/t \leq 0.35$

	ρ/t	0.025	0.050	0.075	0.10	0.15	0.25	0.35
K_{tb}	<i>FEM</i>	2.935	2.353	2.074	1.901	1.689	1.474	1.361
	U&N	2.291	1.970	1.801	1.686	1.531	1.347	1.242
accuracy δ_x		-22.0%	-16.3%	-13.2%	-11.3%	-9.4%	-8.6%	-8.7%

(8), where constants C_1 and C_2 depend on other non-varying characteristic geometrical parameters of the joint.

$$K_{tt} = 1 + C_1(\rho)^{-0.65} \tag{7}$$

$$K_{tt} = 1 + C_2(\rho)^{-0.467} \tag{8}$$

It is worth noting that the exponents in Eqs. (7) and (8) are different, and this means that the stress concentration factors K_{tt} will vary with different rates when the weld toe radius decreases, i.e. when $\rho \rightarrow 0$.

4.2 The plate thickness effect

Another important case occurs when only the thickness t of the main plate varies, while other geometrical parameters of the joint remain unchanged. Such a situation takes place when all weld dimensions depend on constant thickness T of the attachment plate, while the thickness t of the main plate varies. The K_{tt} data obtained for such a case are presented in Fig. 5, where the axial stress concentration factor was obtained for a range of values of parameter X , and it is given as a function of the relative weld throat thickness Y .

In all those cases, the K_{tt} vs. Y relationship can be approximated by a smooth and regular function tending

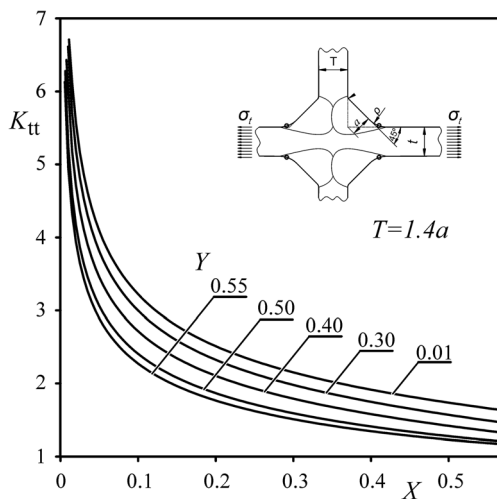


Fig. 4 Influence of the relative weld toe radius X on the axial stress concentration factor K_{tt} obtained for a variety of Y ratios while $T = 1.4a$

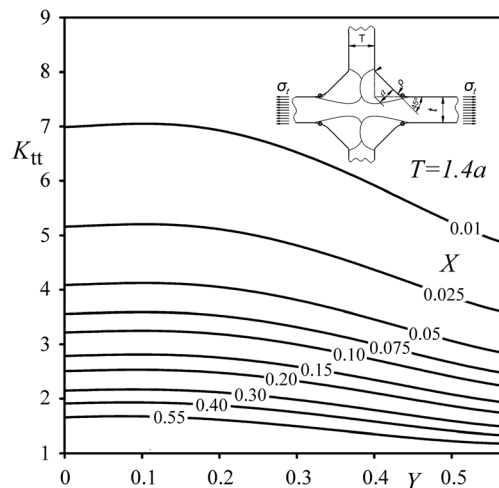


Fig. 5 The effect of the relative thickness Y on the axial stress concentration factor K_{tt} for various X ratios, while $T = 1.4a$

to a finite limit when the relative weld throat thickness Y tends to zero.

When the main plate thickness t increases and the weld toe radius ρ stays constant, the ratio $\rho/t \rightarrow 0$, but the stress concentration factor K_{tt} tends to a finite value and not to infinity, as in the previous case of $\rho \rightarrow 0$.

4.3 Conclusions drawn from finite element method solutions

The analysis of the two cases named as the “radius effect” and the “thickness effect”, presented above, indicates that the ρ/t ratio is a very important parameter influencing stress concentration factors. However, the stress concentration factor K_{tt} depends also on other parameters like the weld throat thickness a and the attachment thickness T . The data presented in Figs. 4 and 5 indicate that when the weld toe radius ρ tends to zero, while the plate thickness t stays constant, the singularity effect occurs, resulting in theoretically infinite stresses at the weld toe. However, when the weld toe radius ρ remains constant, while the main plate thickness t tends to infinity, the maximum stress at the weld toe tends to a finite value. The dual tendency concerning stress concentration factors in welds needs appropriate treatment.

Analogous data and tendencies concerning stress concentration factors under axial load (Figs. 4 and 5) were also obtained under pure bending load. The phenomenon discussed above is illustrated in Fig. 6 for both pure tension (a) and bending load (b), where at least two parameters describing the variation of stress concentration factors in weldments are necessary because the description in terms of only one parameter ρ/t is insufficient.

The data presented in Fig. 6 were obtained with the finite element method by varying the parameters ρ/a and a/t within the range of 0.01 to 1.3.

5 General form of the analytical stress concentration factor formula

The data presented and discussed above indicate that any general mathematical formula for the weldment stress concentration factor requires using an expression capable of modelling the singularity when the weld toe radius ρ tends to zero. It is also necessary to approximate a potential stress concentration factor expression with respect to at least two geometrical parameters such as X and Y defined earlier.

5.1 The sharp corner configuration as the limiting case of the weld toe radius

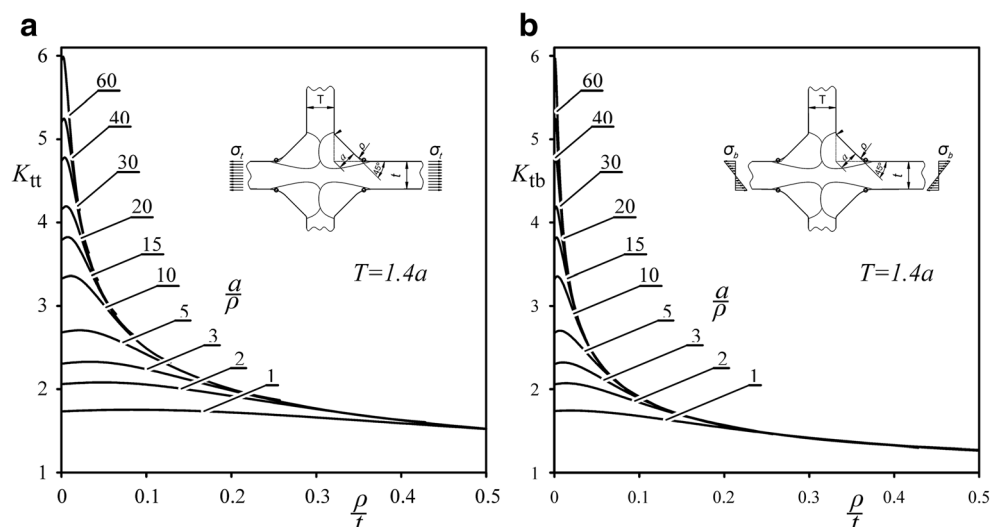
When the weld toe radius $\rho \rightarrow 0$, the weld toe region converts into a sharp corner with its characteristic angle 2α , as shown in Fig. 7.

The fundamental solution to the case [21, 22] shown in Fig. 7 must satisfy the compatibility of the displacement field given by Eq. (9). This means that Eq. (9) must be satisfied for characteristic values of the parameter λ .

$$\sin(2\lambda\alpha) + \lambda\sin(2\alpha) = 0 \quad (9)$$

Since the complimentary angle in the analysed case (weld angle $\theta = 45^\circ$) is $2\alpha = 5\pi/4$, the first characteristic exponent of the solution is $\lambda = 0.6736$. Thus, the degree of the singularity of the fundamental solution is $n = \lambda -$

Fig. 6 Dependence of stress concentration factors as a function of parameters ρ/t , a/ρ while $T/a = 1.4$; **a** variations of K_{tt} under axial load and **b** variations of K_{tb} under bending load



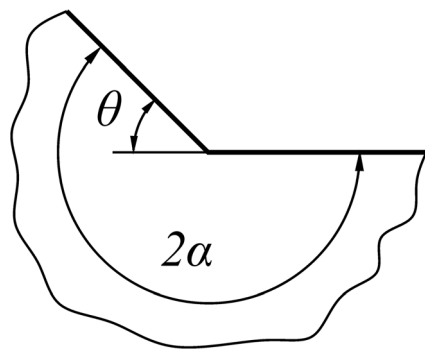


Fig. 7 Sharp corner ($\rho \rightarrow 0$) in a semi-infinite plane and its characteristic angles of 2α and $\theta = 45^\circ$ representing the sharp weld toe region

$1 = -0.3264$. This solution means that as the weld toe radius ρ becomes very small, the stress concentration factor K_{tt} or K_{tb} should be described by the power law function of ρ with the exponent $n = -0.3264$. The singularity of the solution may be subsequently removed by using the K_t/X^n parameter instead of K_{tt} or K_{tb} . As a consequence, a smooth and regular function dependent on parameters X and Y can be obtained for simulating variations of stress concentration factor K_{tt} or K_{tb} . In other words, the stress concentration factor domain can be represented by a surface being the function of parameters X and Y .

5.2 Graphical form of the regular two-dimensional function representing stress concentration factors

Graphical representations of stress concentration factors in the form of surfaces drawn in X and Y coordinates are shown, for axial and bending load, in Fig. 8 and Fig. 9, respectively. The data were obtained with the finite element method for the attachment thickness to the weld throat thickness ratio of $T/a = 1$.

Both surfaces can be easily described by appropriate polynomials involving parameters X and Y varying in the range of

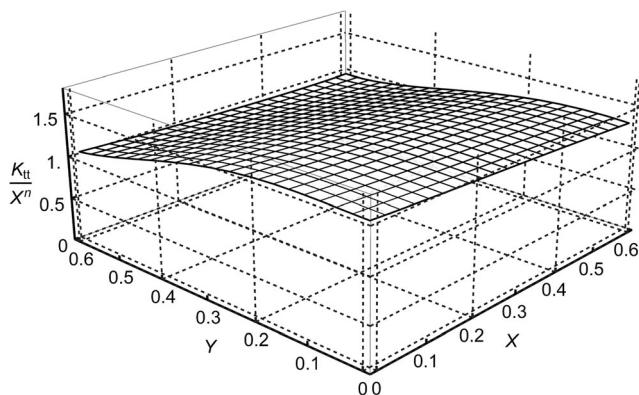


Fig. 8 Regular surface representing the axial stress concentration factor K_{tt} normalised by the singular term; cruciform joint, axial load, $\theta = 45^\circ$, $T/a = 1$, $n = -0.3264$

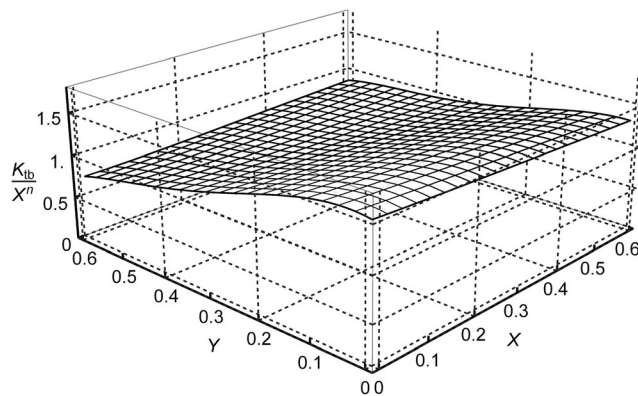


Fig. 9 Regular surface representing the bending stress concentration factor K_{tb} normalised by the singular term; cruciform joint, bending load, $\theta = 45^\circ$, $T/a = 1$, $n = -0.3264$

0 to 0.57. The resulting range of variation for parameters ρ/a and a/t was of 0 to 1.3. It has been concluded that assumed ranges of variation, for all parameters being discussed, were essential and sufficient for practical applications.

The closed form expression for convenient estimation of stress concentration factors in cruciform weldments was selected in the form of Eq. (10)

$$K_t = X^{-0.3264} (A_0 + A_1X + A_2X^2 + A_3X^3 + A_4X^4) \quad (10)$$

The A_i parameters depend only on the non-dimensional geometrical parameter Y . The formula (10) is valid for constant value of parameter $T/a = 1$ involving the thickness of the attachment plate and the weld throat thickness. Parameters A_{it} for the axial and A_{ib} for the bending load are given in the Appendix.

5.3 The effect of the attachment thickness T on stress concentration factors K_{tt} and K_{tb}

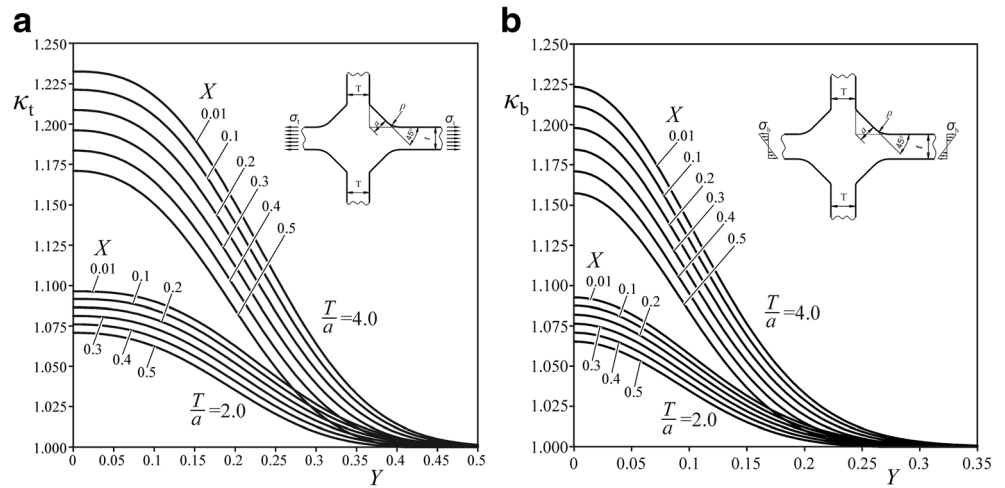
The weld throat thickness a is related to the thickness of one or both plates welded together, and therefore, additional analyses were carried out for relative attachment thicknesses varying in the range of $1 \leq T/a \leq 4$.

The effect of the relative attachment thickness T/a on the stress concentration factors K_{tt} and K_{tb} can be accounted for by introducing two correction functions $\kappa_t(T/a, X, Y)$ and $\kappa_b(T/a, X, Y)$ for tensile and bending load, respectively, given by Eqs. (11) and (12)

$$\kappa_t = 1 + (\sqrt{T/a} - 1) [1 - (0.538 + 8.659Y^2)X] \exp[-(3.654Y)^{2.7} - 1.453] \quad (11)$$

$$\kappa_b = 1 + (\sqrt{T/a} - 1) [1 - (0.600 + 20.148Y^2)X] \exp[-(6.899Y)^{2.0} - 1.492] \quad (12)$$

Fig. 10 Correction functions κ_t and κ_b accounting for the effect of T/a for various X and Y parameters on the stress concentration factors K_{tt} and K_{tb} , respectively, for **a** axial load and **b** bending load



The accuracy of each formula is higher than 99% comparing to *FEM* results.

A range of values of the correction functions κ_t and κ_b for arbitrarily chosen relative attachment thickness $T/a = 2$ and $T/a = 4$ are shown in Fig. 10 a and b for the axial and bending load, respectively.

Thus, the final formulas for the stress concentration factors in cruciform weldments, accounting for the variation of the parameter T/a , can be written down in the form of Eq. (13) and Eq. (14).

$$K_{tt} = X^{-0.3264} (A_{0t} + A_{1t}X + A_{2t}X^2 + A_{3t}X^3 + A_{4t}X^4) \kappa_t(T/a, X, Y) \tag{13}$$

$$K_{tb} = X^{-0.3264} (A_{0b} + A_{1b}X + A_{2b}X^2 + A_{3b}X^3 + A_{4b}X^4) \kappa_b(T/a, X, Y) \tag{14}$$

Particular formulas for calculating numerical values of A_{it} and A_{ib} are given in [Appendix](#).

Table 3 Comparison of K_{tt} values calculated using Eq. (13) (*) to the *FEM* results for a cruciform joint subjected to tensile load, while $T/a = 1.4$

$T/a = 1.4$	$X = \rho/(\rho + a)$					
$Y = a/(a + t)$	0.05	0.15	0.25	0.35	0.45	0.55
0.15	4.105	2.799	2.313	2.022	1.815	1.653
	4.108*	2.799*	2.313*	2.023*	1.816*	1.652*
0.25	3.970	2.700	2.223	1.934	1.726	1.560
	3.950*	2.685*	2.213*	1.928*	1.723*	1.556*
0.35	3.651	2.477	2.034	1.765	1.571	1.416
	3.645*	2.475*	2.035*	1.770*	1.577*	1.421*
0.45	3.269	2.218	1.821	1.581	1.411	1.282
	3.258*	2.211*	1.818*	1.582*	1.413*	1.282*
0.55	2.891	1.964	1.617	1.414	1.277	1.183
	2.891*	1.965*	1.621*	1.419*	1.282*	1.185*

6 Validation of approximating formulas

Numerical *FEM* K_{tt} and K_{tb} values have been compared to their equivalencies obtained by means of the approximating functions. Some examples of such comparisons are presented in Tables 3, 4, 5, and 6, for a cruciform joint subjected to tensile and bending loads.

Accuracy for all approximating formulae and variables in the range of validity, summarised in [Appendix](#), is much better than 97.5%.

7 Conclusions

Extended numerical simulations that were carried out with the help of the *FEM* package ANSYS Mechanical APDL 16.2 have shown that the weld toe radius ρ , the weld throat thickness a and the main plate thickness t are the most important geometrical parameters affecting stress concentration factors

Table 4 Comparison of K_{tb} values calculated using Eq. (14) (*) to the *FEM* results for a cruciform joint subjected to bending load, while $T/a = 1.4$

$T/a = 1.4$	$X = \rho/(\rho + a)$					
$Y = a/(a + t)$	0.05	0.15	0.25	0.35	0.45	0.55
0.15	3.785	2.572	2.118	1.844	1.648	1.504
	3.773*	2.563*	2.112*	1.841*	1.648*	1.497*
0.25	3.266	2.222	1.833	1.604	1.445	1.323
	3.271*	2.226*	1.839*	1.609*	1.448*	1.325*
0.35	2.819	1.931	1.609	1.423	1.299	1.209
	2.819*	1.929*	1.607*	1.421*	1.295*	1.204*
0.45	2.469	1.710	1.443	1.298	1.206	1.143
	2.472*	1.710*	1.445*	1.299*	1.207*	1.143*
0.55	2.178	1.532	1.320	1.209	1.142	1.096
	2.177*	1.530*	1.317*	1.207*	1.139*	1.094*

Table 5 Comparison of K_{tt} values calculated using Eq. (13) (*) to the FEM results for a cruciform joint subjected to tensile load, while $T/a = 3.0$

$T/a = 3.0$	$X = \rho/(\rho + a)$					
$Y = a/(a + t)$	0.05	0.15	0.25	0.35	0.45	0.55
0.15	4.516	3.066	2.519	2.185	1.944	1.751
	4.512*	3.053*	2.507*	2.178*	1.942*	1.754*
0.25	4.189	2.838	2.324	2.009	1.779	1.594
	4.165*	2.815*	2.306*	1.998*	1.774*	1.593*
0.35	3.731	2.525	2.066	1.785	1.580	1.418
	3.707*	2.509*	2.058*	1.784*	1.585*	1.424*
0.45	3.290	2.228	1.826	1.581	1.408	1.278
	3.266*	2.215*	1.821*	1.583*	1.413*	1.281*
0.55	2.893	1.963	1.615	1.410	1.274	1.181
	2.891*	1.965*	1.621*	1.419*	1.282*	1.185*

K_{tt} and K_{tb} of cruciform welded joints having the weld angle $\theta = 45^\circ$. The appropriate description of the singularity appearing when the weld toe radius ρ tends to zero and the introduction of normalising parameters X and Y made the range of application of the final formulae significantly large, i.e. $0 < \rho/a \leq 1.3$, $0 < a/t \leq 1.3$ and $1 \leq T/a \leq 4$ with the maximum percentage error less than 2.5%.

The effect of the relative attachment thickness T/a on K_{tt} and K_{tb} was accounted for by means of two correction functions κ_t and κ_b , given in a close form by Eqs. (11) and (12), which corrected K_{tt} and K_{tb} of a particular reference T/a value to a new actual one. The accuracy of each correction function is about 99% compared to FEM results.

In this way, one general formula (for each loading case) was obtained covering all proportions between geometrical parameters of the cruciform joint commonly used in engineering applications.

Table 6 Comparison of K_{tb} values calculated using Eq. (14) (*) to the FEM results for a cruciform joint subjected to bending load, while $T/a = 3.0$

$T/a = 3.0$	$X = \rho/(\rho + a)$					
$Y = a/(a + t)$	0.05	0.15	0.25	0.35	0.45	0.55
0.15	3.938	2.669	2.190	1.896	1.686	1.528
	3.922*	2.654*	2.177*	1.889*	1.684*	1.524*
0.25	3.289	2.236	1.843	1.608	1.445	1.324
	3.289*	2.236*	1.845*	1.612*	1.449*	1.325*
0.35	2.821	1.933	1.608	1.422	1.297	1.209
	2.820*	1.930*	1.607*	1.421*	1.295*	1.204*
0.45	2.468	1.709	1.444	1.299	1.206	1.142
	2.472*	1.710*	1.445*	1.299*	1.207*	1.143*
0.55	2.177	1.532	1.319	1.209	1.142	1.097
	2.177*	1.530*	1.317*	1.207*	1.139*	1.094*

Since the final solution is given in the form of a polynomial expression, it can be easily applied in computer-aided design processes involving optimisation. The procedure described above may be easily repeated for other types of joints with fillet and butt welds and various weld angles θ .

Appendix. Approximate K_t formulas for a cruciform welded joint subjected to axial and bending load

Variables: ρ, a, t, T

Constant values:

$$\theta = 45^\circ; n = -0.3264$$

Normalising parameters:

$$X = \rho/(\rho + a); Y = a/(a + t)$$

Range of application: $0 < \rho/a \leq 1.3; 0 < a/t \leq 1.3; 1 \leq T/a \leq 4$

Approximation accuracy: maximum percentage error much lower than 2.5% compared with FEM results

General formulas:

$$K_{tt} = X^{-0.3264} (A_{0t} + A_{1t}X + A_{2t}X^2 + A_{3t}X^3 + A_{4t}X^4) \kappa_t \tag{15}$$

$$K_{tb} = X^{-0.3264} (A_{0b} + A_{1b}X + A_{2b}X^2 + A_{3b}X^3 + A_{4b}X^4) \kappa_b \tag{16}$$

Cruciform joint, axial load, $\theta = 45^\circ$

$$\begin{aligned} A_{0t} &= 1.495 + 0.116Y + 1.690Y^2 - 12.878Y^3 + 12.853Y^4 \\ A_{1t} &= -0.405 + 0.553Y - 4.856Y^2 + 12.410Y^3 - 9.082Y^4 \\ A_{2t} &= 0.505 - 0.881Y - 0.405Y^2 + 3.533Y^3 - 2.689Y^4 \\ A_{3t} &= -0.826 + 1.654Y + 5.274Y^2 - 35.138Y^3 + 41.767Y^4 \\ A_{4t} &= 0.374 + 0.061Y - 20.664Y^2 + 79.757Y^3 - 76.234Y^4 \\ \kappa_t &= 1 + \left(\sqrt{T/a} - 1\right) \left[1 - (0.538 + 8.659Y^2)X\right] \exp\left[-(3.654Y)^{2.7} - 1.453\right] \end{aligned}$$

Cruciform joint, bending load, $\theta = 45^\circ$

$$\begin{aligned} A_{0b} &= 1.491 + 1.137Y - 14.897Y^2 + 30.960Y^3 - 21.195Y^4 \\ A_{1b} &= -0.379 - 0.831Y + 5.195Y^2 - 7.152Y^3 + 3.924Y^4 \\ A_{2b} &= 0.440 - 1.322Y + 2.031Y^2 + 4.113Y^3 - 1.144Y^4 \\ A_{3b} &= -0.792 + 2.683Y - 12.341Y^2 + 41.768Y^3 - 55.767Y^4 \\ A_{4b} &= 0.533 - 3.688Y + 25.247Y^2 - 74.895Y^3 + 75.845Y^4 \\ \kappa_b &= 1 + \left(\sqrt{T/a} - 1\right) \left[1 - (0.600 + 20.148Y^2)X\right] \exp\left[-(6.899Y)^{2.0} - 1.492\right] \end{aligned}$$

Open Access This article is licensed under a Creative Commons Attribution 4.0 International License, which permits use, sharing, adaptation, distribution and reproduction in any medium or format, as long as you give appropriate credit to the original author(s) and the source, provide a link to the Creative Commons licence, and indicate if changes were made. The images or other third party material in this article are included in the article's Creative Commons licence, unless indicated otherwise in a credit line to the material. If material is not included in the article's Creative Commons licence and your intended use is not permitted by statutory regulation or exceeds the permitted use, you will need to obtain permission directly from the copyright holder. To view a copy of this licence, visit <http://creativecommons.org/licenses/by/4.0/>.

References

1. Peterson RE (1974) Stress concentration design factors, 2nd edn. Wiley, New York
2. Wilson IH, White DJ (1973) Stress concentration factors for shoulder fillets and grooves in plates. *J Strain Anal* 8:43–51
3. Hasebe N, Sugimoto T, Nakamura T (1987) Stress concentration of longitudinal shear problems. *J Eng Mech* 113:1358–1367
4. Battenbo H, Baines BH (1974) Numerical stress concentration for stepped shafts in torsion in circular and shaped fillets. *J Strain Anal* 9:90–101
5. Abdul-Mihsein MJ, Fenner RT (1985) Some boundary integral equation solutions for three-dimensional stress concentration problems. *J Strain Anal* 20:173–177
6. Noda NA, Takase Y, Monda K (1997) Stress concentration factors for shoulder fillets in round and flat bars under various loads. *Int J Fatigue* 19(1):75–84
7. Zappalorto M, Lazzarin P, Yates JR (2008) Elastic stress distributions for hyperbolic and parabolic notches in round shafts under torsion and uniform antiplane shear loadings. *Int J Solids Struct* 45:4879–4901
8. Fayard JL, Bignonnet A, Dang Van K (1996) Fatigue design criteria for welded structures. *Fatigue Fract Eng Mater Struct* 19(6):723–729
9. Dong P (2001) A structural stress definition and numerical implementation for fatigue analysis of welded joints. *Int J Fatigue* 23(10):865–876
10. Singh PJ, Guha B, Achar DRG (2003) Fatigue life prediction using two stage model for AISI 304L cruciform joints, with different fillet geometry, failing at toe. *Sci Technol Weld Join* 8(1):69–75
11. Balasubramanian V, Guha B (2000) Influence of weld size on fatigue life prediction for flux cored arc welded cruciform joints containing lack of penetration defects. *Sci Technol Weld Join* 5(2):99–104
12. Niemi E (1995) Stress determination for fatigue analysis of welded components. Doc. IIS/IIW-1221-93. Abington Publishing, Cambridge
13. Chattopadhyay A, Glinka G, El-Zein M, Qian J, Formas R (2011) Stress analysis and fatigue of welded structures. *Weld World* 55(7–8):2–21
14. Ushirokawa O, Nakayama E (1983) Stress concentration factor at welded joints. *Ishikawajima-Harima Eng Rev* 23(4):351–355
15. Iida K, Uemura T (1996) Stress concentration factor formulas widely used in Japan. *Fatigue Fract Eng Mater Struct* 19(6):779–786
16. Tsuji I (1990) Estimation of stress concentration factor at weld toe of non-load carrying fillet welded joints. *Trans West Jpn Soc Naval Architects* 80:241–251
17. European Committee for Standardization (CES) (2005) Eurocode 3: Design of steel structures - Part 1–9: Fatigue. Brussels: CES. EN 1993-1-9:2005
18. Young JY, Lawrence FV (1985) Analytical and graphical aids for the fatigue design of weldments. *Fatigue Fract Eng Mater Struct* 8(3):223–241
19. Monahan CC (1995) Early fatigue cracks growth at welds. Computational Mechanics Publications, Southampton
20. Singh PJ, Achar DRG, Guha B, Nordberg H (2002) Influence of weld geometry and process on fatigue crack growth characteristics of AISI 304L cruciform joints containing lack of penetration defects. *Sci Technol Weld Join* 7(5):306–312
21. Williams ML (1952) Stress singularities resulting from various boundary conditions in angular corners of plate in extension. *J Appl Mech* 19:526–528
22. Seweryn A, Molski KL (1996) Elastic stress singularities and corresponding generalized stress intensity factors for angular corners under various boundary conditions. *Eng Fract Mech* 55:529–556

Publisher's note Springer Nature remains neutral with regard to jurisdictional claims in published maps and institutional affiliations.